

72-11

AD 742817

Contract No. DABCO4-69-C-0077  
ARPA Order No. 1442, Amendment 2  
Program Code 9E30

# AN ANALYSIS OF THE STABILITY OF THIN LIQUID FILMS IN HYPERSONIC ENVIRONMENTS

by

John Starkenberg



POLYTECHNIC INSTITUTE OF BROOKLYN

DEPARTMENT  
of  
AEROSPACE ENGINEERING  
and  
APPLIED MECHANICS

APRIL 1972

Reproduced by  
NATIONAL TECHNICAL  
INFORMATION SERVICE  
Springfield, Va. 22151

Unclassified

Security Classification

DOCUMENT CONTROL DATA - R & D

(Security classification of title, body of abstract and indexing annotation must be entered when the overall report is classified)

1. ORIGINATING ACTIVITY (Corporate author) Polytechnic Institute of Brooklyn Dept. of Aerospace Engrg. & Appl. Mechanics Rt. 110, Farmingdale, N.Y. 11735		2a. REPORT SECURITY CLASSIFICATION Unclassified	
3. REPORT TITLE AN ANALYSIS OF THE STABILITY OF THIN LIQUID FILMS IN HYPERSONIC ENVIRONMENTS		2b. GROUP	
4. DESCRIPTIVE NOTES (Type of report and inclusive dates) Research Report			
5. AUTHOR(S) (First name, middle initial, last name) John Starkenberg			
6. REPORT DATE April 1972		7a. TOTAL NO. OF PAGES 34	7b. NO. OF REFS 11
8a. CONTRACT OR GRANT NO. DAHCO4-69-C-0077		9a. ORIGINATOR'S REPORT NUMBER(S) PIBAL REPORT NO. 72-11	
b. PROJECT NO.		9b. OTHER REPORT NO(S) (Any other numbers that may be assigned this report)	
c. ARPA Order No. 1442, Amendment 2			
d. Program Code 9E30			
10. DISTRIBUTION STATEMENT Approved for public release; distribution unlimited.			
11. SUPPLEMENTARY NOTES		12. SPONSORING MILITARY ACTIVITY U.S. Army Research Office-Durham Box CM, Duke Station Durham, North Carolina 27706	
13. ABSTRACT The stability of thin liquid films adjacent to high speed gas flows has been examined to determine its effect on the coolant requirements of hypersonic vehicles. The analysis is also applicable to surface films in high energy exhaust flows. Classical hydrodynamic stability theory was applied to the liquid film with boundary conditions corresponding to both supersonic and subsonic external streams. Instability mechanisms which coupled the disturbance motion of the gas to the disturbance motion of the liquid were of primary interest and those involving energy transfer from the basic flow were specifically excluded. Numerical solutions as well as exact and approximate analytical solutions were developed.  It was determined that there exists a minimum value of the film Reynolds number below which no instabilities may occur in the supersonic case, while in the subsonic case the flow will either be stable or unstable for all coolant Reynolds numbers depending on the value of other flow parameters.			

Unclassified

Security Classification

14. KEY WORDS	LINK A		LINK B		LINK C	
	ROLE	WT	ROLE	WT	ROLE	WT
Liquid film cooling Film cooling Transpiration cooling Hydrodynamic stability Liquid film stability						

Unclassified

AN ANALYSIS OF THE STABILITY OF THIN LIQUID FILMS IN  
HYPERSONIC ENVIRONMENTS

by

John Stassenberg

This research was sponsored by the Advanced Research  
Projects Agency of the Department of Defense and was  
monitored by U.S. Army Research Office-Durham,  
North Carolina under Contract No. DAHCO4-69-C-0077.

POLYTECHNIC INSTITUTE OF BROOKLYN

Department

of

Aerospace Engineering and Applied Mechanics

April 1972

PIBAL Report No. 72-11

AN ANALYSIS OF THE STABILITY OF THIN LIQUID FILMS IN  
HYPERSONIC ENVIRONMENTS<sup>†</sup>

by

John Starckenberg<sup>‡</sup>

Polytechnic Institute of Brooklyn  
Preston R. Bassett Research Laboratory  
Farmingdale, New York

ABSTRACT

The stability of thin liquid films adjacent to high speed gas flows has been examined to determine its effect on the coolant requirements of hypersonic vehicles. The analysis is also applicable to surface films in high energy exhaust flows. Classical hydrodynamic stability theory was applied to the liquid film with boundary conditions corresponding to both supersonic and subsonic external streams. Instability mechanisms which coupled the disturbance motion of the gas to the disturbance motion of the liquid were of primary interest and those involving energy transfer from the basic flow were specifically excluded. Numerical solutions as well as exact and approximate analytical solutions were developed.

It was determined that there exists a minimum value of the film Reynolds number below which no instabilities may occur in the supersonic case, while in the subsonic case the flow will either be stable or unstable for all coolant Reynolds numbers depending on the value of other flow parameters.

---

<sup>†</sup>This research was supported by the Advanced Research Projects Agency of the Department of Defense and was monitored by U.S. Army Research Office-Durham, North Carolina under Contract No. DAHCO4-69-C-0077.

<sup>‡</sup>NASA Fellow.

## TABLE OF CONTENTS

<u>Section</u>		<u>Page</u>
I	Introduction	1
II	Stability Analysis	4
III	Numerical Procedure	17
IV	Presentation and Discussion of Results	20
V	Conclusions	22
VI	References	23

# LIST OF ILLUSTRATIONS

<u>Figure</u>		<u>Page</u>
1	Flow Configuration	24
2a	Behavior of the Eigenfunction, Supersonic Case	25
2b	Behavior of the Eigenfunction, Supersonic Case	26
2c	Behavior of the Eigenfunction, Supersonic Case	27
2d	Behavior of the Eigenfunction, Supersonic Case	28
3	Wave Amplification Vs. Wave Number	29
4	Cut-Off Wave Numbers Vs. Reynolds Number, Supersonic Case	30
5	Amplification Factor Vs. Wave Number, Subsonic Case	31
6	Amplification Factor Vs. Wave Speed for Neutral Stability, Subsonic Case	32
7	Cut-Off Wave Numbers Vs. Reynolds Number, Subsonic Case	33
8	Cut-Off Wave Numbers Vs. $\bar{C}_f$ , Subsonic Case, $R=10$	34

# LIST OF SYMBOLS

$a$	speed of sound
$c_f$	skin friction coefficient
$F$	Froude number
$g$	acceleration due to gravity
$h$	film thickness
$H$	pressure coefficient
$k$	wave number
$m_c$	coolant mass flow rate
$p$	disturbance pressure
$\bar{p}$	static pressure
$R$	liquid film Reynolds number
$T$	surface tension
$u$	disturbance velocity component
$\bar{u}$	total velocity component
$U_t$	interface velocity
$U_e$	external flow velocity
$v$	disturbance velocity component
$\bar{v}$	total velocity component
$W$	Weber number
$\alpha$	non-dimensionalized wave number
$\delta^*$	boundary layer displacement thickness
$\epsilon$	wave amplitude
$\theta$	phase lag
$\mu$	viscosity
$\nu$	kinematic viscosity
$\rho$	density
$\tau$	shear stress



Subscripts

- $l$  liquid film condition
- $e$  external flow condition

## I. INTRODUCTION

The stability of thin liquid films adjacent to slender bodies in high speed gas flows is examined. Maintenance of such films on the external surface of hypersonic vehicles is highly desirable from the standpoint of thermal protection from aerodynamic heating during the re-entry from interplanetary missions. Such a thin cooling film may be established by allowing liquid injected in the stagnation region of the body to be swept downstream covering the surface. The coolant mass flow rate required to effect protection of the vehicle will depend on the surface area and on mass loss due to droplet entrainment and vaporization. The interaction of the gas-liquid interface leads to the formation of surface waves in the liquid film. Depending on the flow conditions, these waves will either be damped (stable film) or will grow with time (unstable film). In the event that the wave amplitudes are not sufficiently decreased with time, droplet entrainment will become the dominant mechanism of mass loss to an extent that an integral layer of liquid will no longer be maintained on the surface.

Coupled with the effect on the liquid film, the presence of waves on the surface also affects the gaseous boundary layer. The flow of a gas over a wavy or "pebbled" surface is similar to flow over a rough surface. These conditions give rise to an increase in the transport of mass, momentum, and energy in the boundary layer and hence an increase in heat transfer and shear stress. The evaporative mass transfer may be considered to consist of the sum of that contribution which would result if the gas-liquid interface were perfectly smooth and the additional contribution due to the effect of the surface roughness. Gater and L'Ecuyer<sup>1</sup> have indicated that this latter effect is independent of the mass flow rate. This, however, ignores the fact that the surface roughness, which is related to the wave amplitude, may be a function of

the mass flow rate. Thus, the effect on changes in the mass flow on the behavior of the interface cannot be disregarded even in attempts to predict mass transfer due to evaporation.

The liquid film cooling phenomenon has been characterized by the existence of a region in which heat is either absorbed by the liquid film, or used to effect a change to the vapor phase, and a region in which cooling is accomplished by heat transfer to the vapor in the boundary layer after the film has been totally vaporized. The effect of an instability occurring at some point on the surface of the vehicle would be to prematurely bring about the reduced cooling effect associated with the total vaporization region.

If an analysis of the stability problem is to be applicable to a given flow system, the probable instability mechanisms of the system must be known so that equations and boundary conditions consistent with these mechanisms may be formulated. The instability mechanisms are of two basic types: those arising due to energy transfer from the basic flow of the gas or liquid, as in Tollmien-Schlichting instabilities and those arising due to energy transfer from the perturbation of the normal and shear stresses induced by the wave formation, such as the pressure perturbation (Kelvin-Helmholtz) and shear perturbation instability mechanisms.

Waves capable of exhibiting the former type of instability were possibly observed by Marshall and Saric<sup>2</sup> in flows of very thin films at relatively high liquid Reynolds numbers. In this case, the wave speed was less than the interface velocity (slow waves) which is a necessary condition for Tollmien-Schlichting instability according to Miles<sup>3</sup>. Most waves observed, however, have not been in this regime.

Craik<sup>4</sup> classified the types of waves observed with an incompressible external air flow which occurred at different values of the film thickness. He found that instabilities may occur for very thin films

while they do not occur for thicker films despite the relatively high damping effect at low Reynolds numbers. He concluded that the dominant mechanism of these instabilities was the action of the shear perturbation which was in phase with the wave slope and tended to pile up liquid at the wave crests.

If the external air flow is compressible, the instability mechanisms related to the pressure disturbance are of different form depending on whether the flow is subsonic or supersonic. For subsonic flow, the disturbance pressure is  $180^\circ$  out of phase with the surface wave amplitude; hence, minimum pressure occurs at the crests and maximum in the troughs, thus drawing liquid to the crests of the waves. However, for supersonic flow, the pressure perturbation is in phase with the wave slope. Chang and Russell<sup>5</sup> and Nachtsheim<sup>6,7</sup> have demonstrated in this case that the dominant mode of energy transfer between the external flow and the perturbations of the liquid flow is through supersonic wave drag.

Chang and Russell performed the stability analysis for a gas-liquid interface including the effects of the perturbations imparted to the gas motion. However, the liquid layer they considered was infinitely deep and initially quiescent. Nachtsheim considered the type of waves observed by Larson and Mateer<sup>8</sup> in the melt layer of a re-entry vehicle. He carried out the analysis for three-dimensional disturbances in thin films adjacent to supersonic flows and showed that the equations may be reduced to two-dimensional form if the wave number and Mach number are appropriately defined. In addition, the experiments of Marshall and Saric suggest that two-dimensional waves occur at intermediate Reynolds numbers. Nachtsheim's work, however, was primarily concerned with the highly viscous melt layer and he concentrated on solutions for vanishingly small Reynolds numbers. In addition, the results he produced were not consistent with any particular external flow but rather were obtained by allowing the non-dimensional parameters in the governing equations

to vary independently.

The present investigation considers thin films at moderate film Reynolds numbers with high speed external flows typical of conditions arising for liquid films in reentry environments. While the free stream Mach numbers in such environments are generally hypersonic, both supersonic and subsonic gas flows are used to provide the perturbation pressure condition at the interface, the former corresponding to a boundary layer much thinner than the disturbance wave amplitude and the latter to a boundary layer which is thick compared to the disturbance amplitude.

For the analysis, instability mechanisms which couple the disturbance motion of the gas to the disturbance motion of the liquid are included, while those involving energy transfer from the basic flow through the action of shear perturbations at the interface or through the action of body forces (Rayleigh-Taylor instabilities), are specifically excluded. The analysis of Nachtsheim is generally followed except that the equation of motion is arrived at from a two-dimensional standpoint and consideration of the vanishingly small Reynolds number regime is excluded. Analytic solutions are also developed. Results based on the numerical and analytic solutions to the equation are presented.

## II. STABILITY ANALYSIS

### (A) The Basic Flow

#### Liquid Film

For the flow of a thin liquid film over a flat solid surface adjacent to a supersonic gas stream and in the absence of perturbations, a very nearly linear velocity profile will be established provided the film is sufficiently thin. The equilibration of shear stress at the interface imposes a velocity on the surface of the liquid film which is

held constant in time and space precluding any energy transfer from the basic flow to the perturbations.

A two-dimensional cartesian coordinate system is introduced such that the x-axis lies in the plane of the interface and the y-axis is perpendicular to that plane and pointing away from the solid wall (see Fig. 1). The basic flow of the liquid is then given by

$$\left. \begin{aligned} \bar{u} &= U_\ell (1 + y/h) \\ \bar{v} &= 0 \\ \bar{p} &= p_e - \rho_\ell g y \end{aligned} \right\} -h \leq y \leq 0 \quad (1)$$

where  $U_\ell$ , the surface velocity, is subject to the condition

$$\mu_\ell U_\ell / h = \tau_g |_{y=0} \quad (2)$$

The gravity vector here is assumed to act in the negative y direction. This is consistent with the linear form of the velocity profile. It should be pointed out, however, that for thin films, the deviations from the linear profile will be small when the gravity vector is arbitrarily directed. Hence, the neglect of the error associated with the application of the following analysis to the general case is consistent with the approximation in the subsequent linearization of the governing equation. However, it must be stipulated that the gravity vector has no component in the positive y direction, in order to preclude instabilities of the Rayleigh-Taylor type.

#### External Gas Flow

The basic flow in the gas is uniform and given by

$$\left. \begin{aligned} \bar{u} &= U_e \\ \bar{v} &= 0 \\ \bar{p} &= p_e \\ \bar{\rho} &= \rho_e \end{aligned} \right\} y \geq 0 \quad (3)$$

The boundary layer is assumed to be very thin compared to the liquid

film depth and its effect is confined to the satisfaction of Eq. (2). The value of the shear stress at the interface may be determined from a boundary layer analysis.

## (B) Disturbance Motion

### Liquid Film

A component of a general harmonic disturbance is now introduced to the motion of the liquid film. The wave-like form of this disturbance is illustrated in Fig. 1. If the x-axis is directed perpendicular to the wave fronts, perturbations normal to the x-y plane will vanish and the total velocity and pressure are given by

$$\begin{aligned}\bar{u} &= U_\ell (1+y/h) + u(y) e^{i(kx-\omega t)} \\ \bar{v} &= v(y) e^{i(kx-\omega t)} \\ \bar{p} &= p_e - \rho_\ell g y + p(y) e^{i(kx-\omega t)}\end{aligned}\tag{4}$$

The wave number  $k$  is assumed to be a real dimensional constant, while the parameter  $\omega$  is taken to be complex. The wave length of the disturbance in the direction of the wave normal is  $2\pi/k$ . The real part of  $\omega$  is the frequency of the disturbance and the imaginary part is the time amplification factor. Hence, the criterion for neutral stability (waves that do not grow or decay with time) is that the imaginary part of  $\omega$  vanish.

### External Gas Flow

A similar disturbance is introduced into the gas flow

$$\begin{aligned}\bar{u} &= U_e + u(y) e^{i(kx-\omega t)} \\ \bar{v} &= v(y) e^{i(kx-\omega t)} \\ \bar{p} &= p_e + p(y) e^{i(kx-\omega t)} \\ \bar{\rho} &= \rho_e + \rho(y) e^{i(kx-\omega t)}\end{aligned}\tag{5}$$

### (C) Disturbance Equations

#### Liquid Film

The equations governing the disturbance amplitude functions are obtained by introducing the velocities and pressure including the perturbation terms into the Navier-Stokes and continuity equations and disregarding non-linear terms in the perturbation quantities on the assumption that the disturbances are small.

$$-i\omega u + U_\ell(1+y/h)iku + vU_\ell/h = -\frac{ik}{\rho_\ell}p + \nu_\ell(u'' - k^2u) \quad (6)$$

$$-i\omega v + U_\ell(1+y/h)ikv = -\frac{1}{\rho_\ell}p' + \nu_\ell(v'' - k^2v) \quad (7)$$

$$iku + v' = 0 \quad (8)$$

Primes here indicate differentiation with respect to  $y$ .

Eliminating  $p$  then  $u$  from Eq. (7) leads to the Orr-Sommerfeld equation for the liquid film

$$\nu_\ell^4 v^{iv} - 2k^2 \nu_\ell^2 v'' + k^4 v = \frac{ik}{\nu_\ell} \{ [U_\ell(1+y/h) - \omega/k] (v'' - k^2 v) \}. \quad (9)$$

and eliminating  $u$  from Eq. (6) leads to the following expression for the disturbance pressure in terms of  $v$  and its derivatives

$$p = \frac{\rho_\ell}{k} \{ i [ (\frac{\omega}{k} - U_\ell(1+y/h)) ] v' + v \frac{U_\ell}{h} + \frac{\nu_\ell}{k} (v'' - k^2 v') \} \quad (10)$$

The disturbance shear stress in the film is

$$\tau_{xy} = \mu_\ell \left( \frac{1}{k} v'' + ikv \right) \quad (11)$$

#### External Gas Flow

The equations of motion for the gas flow are derived in a similar manner. The velocities, pressure and density are introduced into the inviscid momentum equations and the continuity equation for a compressible fluid. Non-linear terms are again neglected.

$$(U_e - \omega/k)u = -\frac{a e^{\beta p}}{\rho_e} \quad (12)$$



$$(U_e - w/k)v = \frac{i}{k} \frac{a_e^2}{\rho_e} \rho' \quad (13)$$

$$(U_e - w/k)i\rho = -\rho_e(iu - v'k) \quad (14)$$

Elimination of  $\rho$  and  $u$  from the governing equation leads to the following equation

$$v'' + k^2 \left[ \frac{(U_e - w/k)^2}{a_e^2} - 1 \right] v = 0 \quad (15)$$

Eliminating  $u$  from Eq. (12) and using the relation  $p = a_e^2 \rho$  yields the following expression for the pressure

$$p = \frac{i\rho_e(U_e - w/k)v'}{k \left[ \frac{(U_e - w/k)^2}{a_e^2} - 1 \right]} \quad (16)$$

The shear stress in the gas is zero. The specification of this condition rules out the shear stress instability mechanism.

Now for  $U_e \gg w/k$

$$v'' + k^2(M_e^2 - 1)v = 0 \quad (17)$$

The supersonic solution to this equation is valid for  $M_e > 1$ .

#### (D) Boundary Conditions

The boundary conditions to be imposed on the equation for the liquid film at the interface are that the discontinuity in normal stress be equilibrated by the surface tension and that the tangential stress be continuous. The no-slip condition is imposed at the wall.

The conditions in the gas may be determined analytically from Eq. (17). The boundary conditions for Eq. (17) are the kinematic condition at the interface and that the velocity remain finite as  $y \rightarrow \infty$ . The equation of the interface is

$$\bar{y} = \epsilon e^{i(kx - \omega t)} \quad (18)$$

and the kinematic condition is

$$\bar{v} = \frac{\partial \bar{y}}{\partial t} + \bar{u} \frac{\partial \bar{y}}{\partial x} \quad (19)$$

In terms of perturbation quantities

$$v = ikU_e \epsilon \quad (20)$$

The solution to Eq. (17) subject to boundary condition (20) is

$$v = ikU_e \epsilon e^{ik\sqrt{M_e^2-1} y} \quad (21)$$

Now  $\epsilon$  may be determined from the kinematic condition for the liquid at the interface

$$v = ik(U_l - \omega/k) \epsilon$$

Then the disturbance pressure in the gas, Eq. (16) reduces to

$$p = \frac{\rho_\infty U_e^2 v}{(U_l - \omega/k) \sqrt{M_e^2-1}} \quad (22)$$

in the supersonic case and to

$$p = \frac{i \rho_\infty U_e^2 v}{(U_l - \omega/k) \sqrt{1-M_e^2}} \quad (23)$$

in the subsonic case.

Thus, the condition on the normal stress at the interface in the supersonic and subsonic cases are given, respectively, by

$$\begin{aligned} \frac{iv_l}{k} v''' + [(U_l - \omega/k) - 3iv_l k] v' - \frac{U_l}{h} v \\ = \frac{1}{\rho_l} (Tk^2 + \rho_l g + \frac{ik \rho_e U_e^2}{\sqrt{M_e^2-1}}) \left( \frac{v}{U_l - \omega/k} \right) \end{aligned} \quad (24)$$

and

$$\begin{aligned} \frac{iv_l}{k} v''' + [(U_l - \omega/k) - 3iv_l k] v' - \frac{U_l}{h} v \\ = \frac{1}{\rho_l} (Tk^2 + \rho_l g - \frac{k \rho_e U_e^2}{\sqrt{1-M_e^2}}) \left( \frac{v}{U_l - \omega/k} \right) \end{aligned} \quad (25)$$

If the disturbance shear stress in the gas is neglected, the boundary condition becomes

$$v'' + k^2 v = 0 \quad \text{at } y = 0 \quad (26)$$

The condition at the wall is that the velocity vanish

$$v = v' = 0 \quad \text{at } y = -h \quad (27)$$

#### (E) Dimensionless Form of Equations

The variables may be non-dimensionalized as follows

$$\eta = y/h$$

$$\phi(\eta) = v(y)/U_t$$

Equation (9) and the boundary conditions (24), (25), (26) and (27) are transformed to

$$\phi^{iv} - 2\alpha^2 \phi'' + \alpha^4 \phi = i\alpha R[(1+\eta-c)(\phi'' - \alpha^2 \phi)] \quad (28)$$

at  $\eta = 0$

$$\frac{i}{\alpha R} \phi''' + [(1-c) - \frac{3i\alpha}{R}] \phi' - \phi = (\frac{\alpha^2}{W^2} + \frac{1}{F^2} + H) \frac{\phi}{1-c} \quad (29)$$

$$\phi'' + \alpha^2 \phi = 0 \quad (30)$$

at  $\eta = -1$

$$\phi = \phi' = 0 \quad (31)$$

where primes now denote differentiation with respect to  $\eta$  and

$$c = \frac{w/k}{U_t}$$

$$\alpha = kh$$

$$R = \frac{U_t h}{\nu_t}$$

$$c_f = \frac{2\mu_t U_t}{h \rho_e U_e^2}$$

$$F = \frac{U_t}{\sqrt{gh}}$$

$$W = U_t \sqrt{\frac{\rho h}{T}}$$

$$H = \frac{i\alpha}{c_f R \sqrt{M_e^2 - 1}} \quad (\text{supersonic})$$

$$H = \frac{-\alpha}{c_f R \sqrt{1 - M_e^2}} \quad (\text{subsonic})$$

If the function  $\varphi$  is defined such that

$$\varphi(\eta) = \bar{\varphi}(\eta)/\bar{\varphi}(0) = v(y)/v(0) \quad (32)$$

the equations and boundary conditions will retain their same form as follows:

$$\varphi^{iv} - 2\alpha^2 \varphi'' + \alpha^4 \varphi = i\alpha R[(1+\eta-c)(\varphi'' - \alpha^2 \varphi)] \quad (33)$$

at  $\eta = 0$

$$\frac{i}{\alpha R} \varphi''' + [(1-c) - \frac{3i\alpha}{R}] \varphi' - \varphi = (\frac{\alpha^2}{W^2} + \frac{1}{F^2} + H) \frac{\varphi}{1-c} \quad (34)$$

$$\varphi'' + \alpha^2 \varphi = 0 \quad (35)$$

at  $\eta = -1$

$$\varphi = \varphi' = 0 \quad (36)$$

with the additional condition that

$$\varphi = 1 \quad \text{at } \eta = 0 \quad (37)$$

Noting that the combination  $\varphi^{(n)} - \alpha^2 \varphi^{(n-2)}$ , appears repeatedly in the equation, a new function  $\psi$  may be defined

$$\psi = \varphi'' - \alpha^2 \varphi \quad (38)$$

The equation may now be reduced to a system of two second-order equations

$$\varphi'' = \alpha^2 \varphi + \psi \quad (39)$$

$$\psi'' - \alpha^2 \psi = i\alpha R(1+\eta-c)\psi$$

and the boundary conditions

at  $\eta = 0$

$$\psi' = 2\alpha^2 \varphi' - i\alpha \left\{ \left[ R \left( \frac{\alpha^2}{W^2} + \frac{1}{F^2} + H \right) \right] \frac{1}{c-1} - R[(c-1)\varphi' + 1] \right\} \quad (40)$$

$$\psi + 2\alpha^2 \varphi = 0 \quad (41)$$

and at  $\eta = -1$

$$\varphi = \varphi' = 0 \quad (42)$$

The above equations and boundary conditions constitute an eigenvalue problem. The eigenvalue consists of  $\text{Re}\{c\}$ , the non-dimensionalized wave speed and  $\text{Im}\{c\}$ , the time amplification factor. If the eigenvalue is correctly chosen, the homogeneous boundary condition (40) will be satisfied independent of the choice of the initial value of  $\varphi$ . This is illustrated by the fact that the equations retain the same form under the transformation (32) which is equivalent to the choice of initial condition (37).

For a given liquid and gas, the problem is completely specified by the geometry, mass flow rate, and the balance of shear stress for the basic flow. Geometric considerations, in general, lead to an expression for the mass flow of the form

$$m_c = m_c(U_l h) = f(\text{geom})R$$

and from the condition on the shear stress

$$\tau_{\eta=0} = \mu_l \left( \frac{U_l}{h} \right) = c_f \rho_e U_e^2$$

Thus, the interface velocity and film thickness are specified for a given mass flow and external gas flow.

#### (F) Analytic Solution for Small Values of $\alpha$

If the boundary condition (40) is to remain well behaved at  $c=1$ , then  $\alpha$  must be equal to zero for  $c=1$ . Hence, solutions are sought for vanishingly small  $\alpha$  with  $c$  near 1. The parameter  $c$  and the dependent variables  $\varphi$  and  $\psi$  are expressed as a series in powers of  $\alpha$

$$c = 1 + c_1 \alpha + c_2 \alpha^2 + c_3 \alpha^3 + \dots$$

$$\varphi = \varphi_0 + \varphi_1 \alpha + \varphi_2 \alpha^2 + \varphi_3 \alpha^3 + \dots$$

$$\psi = \psi_0 + \psi_1 \alpha + \psi_2 \alpha^2 + \psi_3 \alpha^3 + \dots$$

Substitution into the differential equations yields to zeroth order in  $\alpha$

$$\begin{aligned}\varphi_0'' &= \psi_0 \\ \psi_0'' &= 0\end{aligned}\tag{43}$$

with the boundary conditions

at  $\eta = 0$

$$\begin{aligned}\varphi_0 &= 1 \\ \psi_0 &= 0\end{aligned}\tag{44}$$

$$\psi_0' = \frac{iR}{c_1 F^3}$$

at  $\eta = -1$

$$\varphi_0 = 0\tag{45}$$

$$\varphi_0' = 0$$

the solution for  $\varphi_0$  and  $\psi_0$  are

$$\varphi_0 = -\frac{1}{2}\eta^3 + \frac{3}{2}\eta + 1\tag{46}$$

$$\psi_0 = -3\eta$$

and from the extra condition at  $\eta = 0$

$$c_1 = \frac{-iR}{3F^3}\tag{47}$$

retaining first order terms in  $\alpha$  leads to the following equations and boundary conditions in the supersonic case

$$\begin{aligned}\varphi_1'' &= \psi_1 \\ \psi_1'' &= -3iR\eta^3\end{aligned}\tag{48}$$

at  $\eta = 0$

$$\varphi_1 = 0$$

$$\psi_1 = 0\tag{49}$$

$$\psi_1' = \frac{-1}{c_1 c_F M_e^3 - 1} - \frac{ic_2 R}{c_1 F^3} - iR$$

at  $\eta = -1$

$$\begin{aligned}\varphi_1 &= 0 \\ \varphi_1' &= 0\end{aligned}\quad (50)$$

and the solution

$$\begin{aligned}\varphi_1 &= \frac{-iR}{120}\eta^6 - \frac{iR}{48}\eta^3 + \frac{iR}{80}\eta \\ \psi_1 &= \frac{-iR}{4}\eta^4 - \frac{iR}{8}\eta\end{aligned}\quad (51)$$

and again from the extra condition at  $\eta = 0$

$$c_2 = \frac{7R^2}{72F^2} + \frac{1}{3c_f\sqrt{M_e^2-1}}\quad (52)$$

If second order terms in  $\alpha$  are retained, the following solutions result

$$\begin{aligned}\varphi_2 &= \frac{R^2}{12096}\eta^9 + \frac{R^2}{2880}\eta^6 + \frac{1}{20}\left(\frac{R^2}{6F^2} - 1\right)\eta^5 + \frac{1}{6}\left(K + \frac{3}{2}\right)\eta^3 + \frac{\eta^2}{2} + L\eta \\ \psi_2 &= \frac{R^2}{168}\eta^7 + \frac{R^2}{96}\eta^4 + \frac{1}{6}\left(\frac{R^2}{F^2} - 3\right)\eta^3 + K\eta - 2\end{aligned}\quad (53)$$

where

$$\begin{aligned}K &= \left(\frac{1}{192} - \frac{1}{504}\right)R^2 - \frac{9R^2}{10F^2} - \frac{12}{5} \\ L &= \left(\frac{1}{480} + \frac{1}{1008} - \frac{1}{1344} - \frac{1}{384}\right)R^2 - \frac{R^2}{120F^2} - \frac{3}{10}\end{aligned}\quad (54)$$

and

$$c_3 = iR\left[\left(\frac{1}{4536} + \frac{1}{36} - \frac{2}{45F^2}\right)\frac{R^2}{F^2} - \frac{1}{3W^2} + \frac{13}{30F^2} + \frac{7}{72c_f\sqrt{M_e^2-1}}\right]\quad (55)$$

Thus,

$$\begin{aligned}c &= 1 - \frac{iR}{3F^2}\alpha + \left(-\frac{7R^2}{72F^2} + \frac{1}{3c_f\sqrt{M_e^2-1}}\right)\alpha^2 \\ &\quad + iR\left[\left(\frac{1}{4536} + \frac{1}{36} - \frac{2}{45F^2}\right)\frac{R^2}{F^2} - \frac{1}{3W^2} + \frac{13}{30F^2} + \frac{7}{72c_f\sqrt{M_e^2-1}}\right]\alpha^3 + \dots \\ \varphi(\eta) &= -\frac{1}{2}\eta^3 + \frac{3}{2}\eta + 1 - \frac{iR}{8}\left(\frac{\eta^6}{15} + \frac{\eta^3}{6} - \frac{\eta}{10}\right)\alpha \\ &\quad + \left[\frac{R^2}{12096}\eta^9 + \frac{R^2}{2880}\eta^6 + \frac{1}{20}\left(\frac{R^2}{6F^2} - 1\right)\eta^5 + \frac{1}{6}\left(K + \frac{3}{2}\right)\eta^3 + \frac{\eta^2}{2} + L\eta\right]\alpha^2 + \dots\end{aligned}\quad (56)$$

(57)

If the same procedure is carried out in the subsonic case, the resulting expression for  $c$  is

$$c = 1 - \frac{iR}{3F^2} \alpha + \left( \frac{7R^2}{72F^2} + \frac{i}{3c_f \sqrt{1-M_e^2}} \right) \alpha^2 + iR \left[ \left( \frac{1}{4536} + \frac{1}{36} + \frac{2}{45F^2} \right) \frac{R^2}{F^2} - \frac{1}{3W^2} + \frac{13}{30F^2} \right] - \frac{7R}{72c_f \sqrt{1-M_e^2}} \alpha^3 \quad (58)$$

with no change in the expression for  $\phi$ .

Note that the expression for  $c$  indicates that  $\alpha=0$  corresponds to neutral stability in either case.

#### (G) Exact Subsonic Solution

In the subsonic case a simple analytic solution giving the cut-off wave numbers (for which  $\text{Im}\{c\}=0$ ) may be obtained when neutral stability implies  $c=1$ . In the subsonic case,  $H$  is real and negative. Hence, the term in brackets multiplying  $1/(c-1)$  in the boundary condition (40) may vanish and must do so as  $c$  approaches unity. Therefore, the cut-off wave numbers may be determined from the expression

$$\frac{\alpha_N^2}{W^2} + \frac{1}{F^2} - \frac{\alpha_N}{c_f R \sqrt{1-M_e^2}} = 0 \quad (59)$$

The following values of  $\alpha_N$  are obtained

$$\alpha_{N1,2} = \frac{W^2}{2c_f R \sqrt{1-M_e^2}} \pm \sqrt{\left( \frac{W^2}{2c_f R \sqrt{1-M_e^2}} \right)^2 - \left( \frac{W^2}{F^2} \right)} \quad (60)$$

#### (H) Remarks on the Applicability of Subsonic and Supersonic Solutions - Boundary Layer Effects

While the present investigation is concerned exclusively with situations in which the external gas stream is supersonic, the subsonic solutions may also be of interest. Nachtsheim has suggested that the basic flow in the gas may be regarded as a "suitable mean" of an actual boundary layer flow. However, the presence of the gaseous boundary layer will influence the phase lag of the pressure perturbation at the



interface as well as the appropriate values of the Mach number and "free stream" velocity. Indeed, the subsonic solution may be valid for a flow with a supersonic external stream when the boundary layer is thick enough to attenuate the pressure perturbations in the subsonic region.

In the limit of an infinitely thin boundary layer with a supersonic external stream, the pressure perturbation is seen to exhibit a  $90^\circ$  phase lag with respect to the surface wave amplitude while the Mach number appropriately assumes the free stream value. In the opposing limit, as the boundary layer thickness becomes large compared to the wave amplitude, the external flow may be regarded as subsonic for which a  $180^\circ$  phase lag occurs. Hence, as the ratio of boundary layer thickness to wave amplitude varies between the two limits, it is to be expected that the phase lag will vary between  $90^\circ$  and  $180^\circ$ . This behavior has been amply demonstrated experimentally by Muhlstein and Beranek<sup>9</sup>.

In order to take this effect into account, the pressure coefficient at the interface,  $H$ , could be expressed as follows:

$$H = \frac{\alpha}{c_f R \sqrt{|M_e^2 - 1|}} e^{i\theta}$$

where  $\theta$  is the phase lag. This clearly reduces to the supersonic case when  $\theta=90^\circ$  and to the subsonic case when  $\theta=180^\circ$ . Here  $\theta$ ,  $c_f$  and  $M_g$  would be functions of  $\delta^*/\epsilon$ . The difficulty in applying this approach lies in making an appropriate choice for the parameter values. The results of Muhlstein and Beranek indicate that it is sometimes reasonable to use the limiting values of  $\theta$  (particularly in the subsonic case) when  $\delta^*/\epsilon$ ,  $c_f$  and  $M_g$  are not very near their limiting values.

Therefore, the approach here will be to employ the strictly supersonic and subsonic phase lags in the analysis. The problem of choosing parameter values is not clearly resolved, although reasonable

choices may be made.

### III. NUMERICAL PROCEDURE

Since the parameters  $R$ ,  $c_f$ ,  $F$ ,  $W$ , and  $M_e$  are specified for a given liquid mass flow and given external flow, it is necessary to determine the eigenvalue  $c$  as a function of  $\alpha$  satisfying the equations and boundary conditions. Thus, for any  $\alpha$ , a numerical procedure may be used to determine the values of  $c$  for which Eq. (39) has solutions satisfying the boundary conditions (40)-(42).

In order to carry out a numerical integration of the equations starting at  $\eta=0$ , an initial guess for the eigenvalue  $c$  and two additional conditions are required. The initial conditions may be expressed in the form

$$\begin{aligned}\varphi(0) &= A \\ \varphi'(0) &= B\end{aligned}\tag{61}$$

As previously noted, solutions satisfying the boundary conditions are completely independent of the choice of the initial condition on  $\varphi$ . Therefore,  $A$  is taken to be 1 as in the analytic solution. The value of  $B$ , therefore, must be determined from the boundary conditions. For small values of  $\alpha$ , Eq. (57) differentiated with respect to  $\eta$  and evaluated at  $\eta=0$  may be used to obtain an initial guess for  $B$  and Eq. (56) or Eq. (58) may be used to find  $c$ . The formulated initial conditions (40) and (41) may then be written in terms of the assumed initial condition as follows:

$$\begin{aligned}\psi &= -2\alpha^2 \\ \psi' &= 2\alpha^3 B + i\alpha \left\{ \left[ R \left( \frac{\alpha^2}{W^2} + \frac{1}{F^2} + H \right) \right] \frac{1}{c-1} + R[(c-1)B + 1] \right\}\end{aligned}\tag{62}$$

The equations are then integrated from  $\eta=0$  to  $\eta=-1$  and the solutions are checked to see if the conditions at the solid surface are satisfied. Since  $\varphi$  and  $\varphi'$  must both vanish at  $\eta=-1$ , the sum of their

absolute values constitutes the error corresponding to any guess for  $c$  and  $B$ . If the boundary conditions are not satisfied to within the accuracy of the integration,  $c$  and  $B$  must be adjusted accordingly.

In order to facilitate the rapid convergence to a satisfactory solution, it is helpful to know how  $\varphi$  and  $\psi$  vary with  $B$  and  $c$  at  $\eta = -1$ . Differential equations for  $\varphi_B$ ,  $\varphi_B'$ ,  $\varphi_c$  and  $\varphi_c'$ , where subscripts indicate differentiation, may be obtained by differentiating the Eqs. (39) and initial conditions (61) and (62) with respect to  $B$  and  $c$ . The resulting equations and initial conditions are:

$$\begin{aligned}\varphi_B'' &= \alpha^2 \varphi_B + \psi_B \\ \psi_B'' &= \alpha^2 \psi_B + i\alpha R(1 + \eta - c)\psi_B \\ \varphi_c'' &= \alpha^2 \varphi_c + \psi_c \\ \psi_c'' &= \alpha^2 \psi_c + i\alpha R(1 + \eta - c)\psi_c - i\alpha R\psi\end{aligned}\quad (63)$$

at  $\eta = 0$

$$\begin{aligned}\varphi_B &= 0 \\ \varphi_B' &= 1 \\ \psi_B &= 0 \\ \psi_B' &= 2\alpha^2 - i\alpha R(c-1)\end{aligned}\quad (64)$$

$$\begin{aligned}\varphi_c &= 0 \\ \varphi_c' &= 0 \\ \psi_c &= 0 \\ \psi_c' &= -i\alpha \left\{ \left[ R \left( \frac{1}{F^2} + \frac{\alpha^2}{W^2} + H \right) \right] \frac{1}{c-1} + RB \right\}\end{aligned}\quad (65)$$

The adjustments  $\Delta B$  and  $\Delta c$  to the  $i$ th guess are obtained from the Newton-Raphson equations:

$$\begin{aligned}\varphi_{i+1}(-1) &= \varphi_i(-1) + \varphi_{B_i}(-1)\Delta B + \varphi_{c_i}(-1)\Delta c = 0 \\ \varphi_{i+1}'(-1) &= \varphi_i'(-1) + \varphi_{B_i}'(-1)\Delta B + \varphi_{c_i}'(-1)\Delta c = 0\end{aligned}\quad (66)$$

A program incorporating the above numerical approach was run on the IBM 360/50 computer at the Polytechnic Institute of Brooklyn and on the remote terminal of the CDC 6600 computer located at the Preston R. Bassett Research Laboratory.

The numerical integration was carried out using the fourth order Runge-Kutta subroutine, RKGS, taken from the IBM system/360 Scientific Subroutine Package. This subroutine allows the programmer to specify the tolerable integration error and adjusts the step size until this specification is met. In order to make use of this subroutine, it was necessary to recast the equation in terms of real variables and reduce them to first order. This led to a system of twenty-four first order linear differential equations. The eigenvalue and initial conditions were adjusted by the Newton-Raphson technique until the error defined by the sum of absolute values of  $\phi(-1)$  and  $\phi'(-1)$  was zero to within the accuracy of integration. This usually meant less than  $5 \times 10^{-6}$ .

After this technique had converged to an eigenvalue,  $\alpha$  was incremented and the corresponding new eigenvalue was obtained. This procedure was continued using a second degree extrapolation to predict the new eigenvalue and initial condition.

It was found that an increasingly accurate initial guess was required to insure convergence to the proper eigenvalue as  $\alpha$  was increased. As a consequence, it was necessary to keep the increment of  $\alpha$  very small. A highly accurate initial guess is also desired since the integration procedure is time consuming and less rapid advancement in  $\alpha$  is preferable to permitting numerous iterations of the integration. In addition, the possibility of convergence to an extraneous eigenvalue exists if care is not taken in selecting the first approximation to the eigenvalues and initial conditions. The behavior of the eigenfunctions for two values of  $\alpha$  is illustrated in Fig. 2. Typically, the curvature of these functions increases with increasing  $\alpha$  and thus the computation

time becomes significantly greater. In some cases this curvature was sufficiently large that an inordinately small step size was required and the integration procedure failed. When these cases were rerun with a relaxation in the accuracy criterion, such that the solution could be obtained, it appeared that the eigenvalues obtained were relatively insensitive to the accuracy requirement.

#### IV. PRESENTATION AND DISCUSSION OF RESULTS

##### (A) Flow Conditions

The external flow conditions used are given in the following table.

	$M_g$	$c_f$	$c_{f\sqrt{ M_e^2-1 }}$
Free Stream	2.00		
Supersonic Case	2.00	.0115	.020
Subsonic Case	0.25	.0264	.020

The Weber and Froude numbers consistent with a surface shear stress of .005 psi are given by

$$W = .04958R^{3/4}$$

$$F = 23.793R^{1/4}$$

##### (B) Supersonic Case

The behavior of  $c$  as a function of  $\alpha$  is plotted in Fig. 3 for several values of the Reynolds number. There are characteristically two cut-off wave numbers other than  $\alpha = 0$ . It is possible to use Eq. (56) to determine the first cut-off wave number,  $\alpha_{N_1}$ , when the coefficient of  $\alpha^3$  is positive.

In Fig. 4 the cut-off wave numbers are plotted versus Reynolds number. Most striking about their behavior is that there exists a minimum Reynolds number below which no instabilities occur for any wave

number. This can be attributed to that fact that for small Reynolds number the stabilizing effect of the surface tension becomes dominant. That is, in the boundary condition (40) the term  $\alpha^2/W^2$  dominates for small  $R$ . Further, since the stabilizing term  $1/F^2$  dominates for large  $R$ , it might be expected that there exists a maximum Reynolds number above which all wave numbers are stable. However, it has not been possible to demonstrate that here. Results obtained in previous publications which ignored the necessary  $R$  dependence of  $F$  and  $W$  have predicted such a maximum Reynolds number, but these results must be regarded as inapplicable to real systems. Flows for which there are no values of  $\alpha$  for which  $I_m\{c\} > 0$  may be regarded as generally stable.

#### (C) Subsonic Case

Comparison of the analytic and numerical solutions indicates that the former is exact for all values of  $R$ . The numerically obtained plot of amplification factor versus wave number is displayed in Fig. 5 from which the two characteristic cut-off wave numbers are evident. In addition, the wave speed is seen to be smaller than unity in the unstable region. This behavior is also clear in Fig. 6 where  $c$  is plotted in the complex plane. For all values of  $R$ ,  $c=1$  at neutrally stable values of  $\alpha$ ,  $c < 1$  at unstable values of  $\alpha$  and  $c > 1$  at stable values of  $\alpha$ . As  $\alpha$  is increased, starting at the first cut-off, the branches are traversed in a counter-clockwise manner. This effect rather than the Tollmien-Schlichting instability mechanism may explain the slow waves observed by Marshall and Saric. It is notable that these waves were observed only in the thinnest films considered for which the ratio of boundary layer displacement thickness to wave amplitude was greatest.

The  $\alpha$ - $R$  diagram presented in Fig. 7 indicates that no finite maximum or non-zero minimum Reynolds numbers exist beyond which there are no unstable wave numbers. This is generally true for values of

$\bar{c}_f$  below some maximum as indicated in Fig. 8. Thus, such flows are generally unstable when  $\bar{c}_f$  lies below the maximum and stable when  $\bar{c}_f$  lies above the maximum.

## V. CONCLUSIONS

The following general conclusions may be drawn from the present results when the pressure perturbation instability mechanism is predominant. For some values of the Reynolds number, no instabilities will occur when the phase lag is  $180^\circ$ . For boundary layer flows where  $\theta$  is less than  $180^\circ$  the effect of approaching  $\theta=90^\circ$  may be regarded as stabilizing. As the unstable slow waves grow in the boundary layer, the effect is to retard the appropriate phase lag and stabilize the motion for certain values of  $R$ . In this manner, steady amplitude, fast or slow waves may be produced without non-linear effects.

## VI. REFERENCES

1. Gater, R.A. and L'Ecuyer, M.R.: A Fundamental Investigation of the Phenomena that Characterize Liquid Film Cooling. Purdue University Report TM-69-1, January 1969.
2. Marshall, B.W. and Saric, W.S.: An Experimental Investigation of the Stability of a Thin Liquid Layer Adjacent to a Supersonic Stream. AIAA Paper No. 70-801, 1970.
3. Miles, J.W.: The Hydrodynamic Stability of a Thin Film of Liquid in Uniform Shearing Motion. J. Fluid Mech., Vol. 8, Part 4, pp. 593-610, 1960.
4. Craik, A.D.D.: Wind-Generated Waves in Thin Liquid Films. J. Fluid Mech., Vol. 26, Part 2, pp. 369-392, 1966.
5. Chang, I.D. and Russell, P.E.: Stability of a Liquid Layer Adjacent to a High Speed Gas Stream. Phys. Fluids, Vol. 8, No. 6, pp. 1018-1026, 1965.
6. Nachtsheim, P.R.: Analysis of the Stability of a Thin Liquid Film Adjacent to a High-Speed Gas Stream. NASA TN D-4976, January 1969.
7. Nachtsheim, P.R.: Stability of Crosshatched Wave Patterns in Thin Liquid Films Adjacent to Supersonic Streams. Phys. Fluids, Vol. 13, No. 10, pp. 2432-2447, 1970.
8. Larson, H.K. and Mateer, G.G.: Crosshatching - A Coupling of Gas Dynamics with the Ablation Process. AIAA Paper No. 68-670, 1968.
9. Muhlstein, L. and Beranek, R.G.: Experimental Investigation of the Influence of the Turbulent Boundary Layer on the Pressure Distribution Over a Rigid Two-Dimensional Wavy Wall. NASA TN D-6477, August 1971.
10. Betchov, R. and Criminale, W.O.: Stability of Parallel Flows. Academic Press, New York, 1967.
11. Liepmann, H.W. and Roshko, A.: Elements of Gas Dynamics. John Wiley and Sons, Inc. New York, pp. 208-215, 1967.



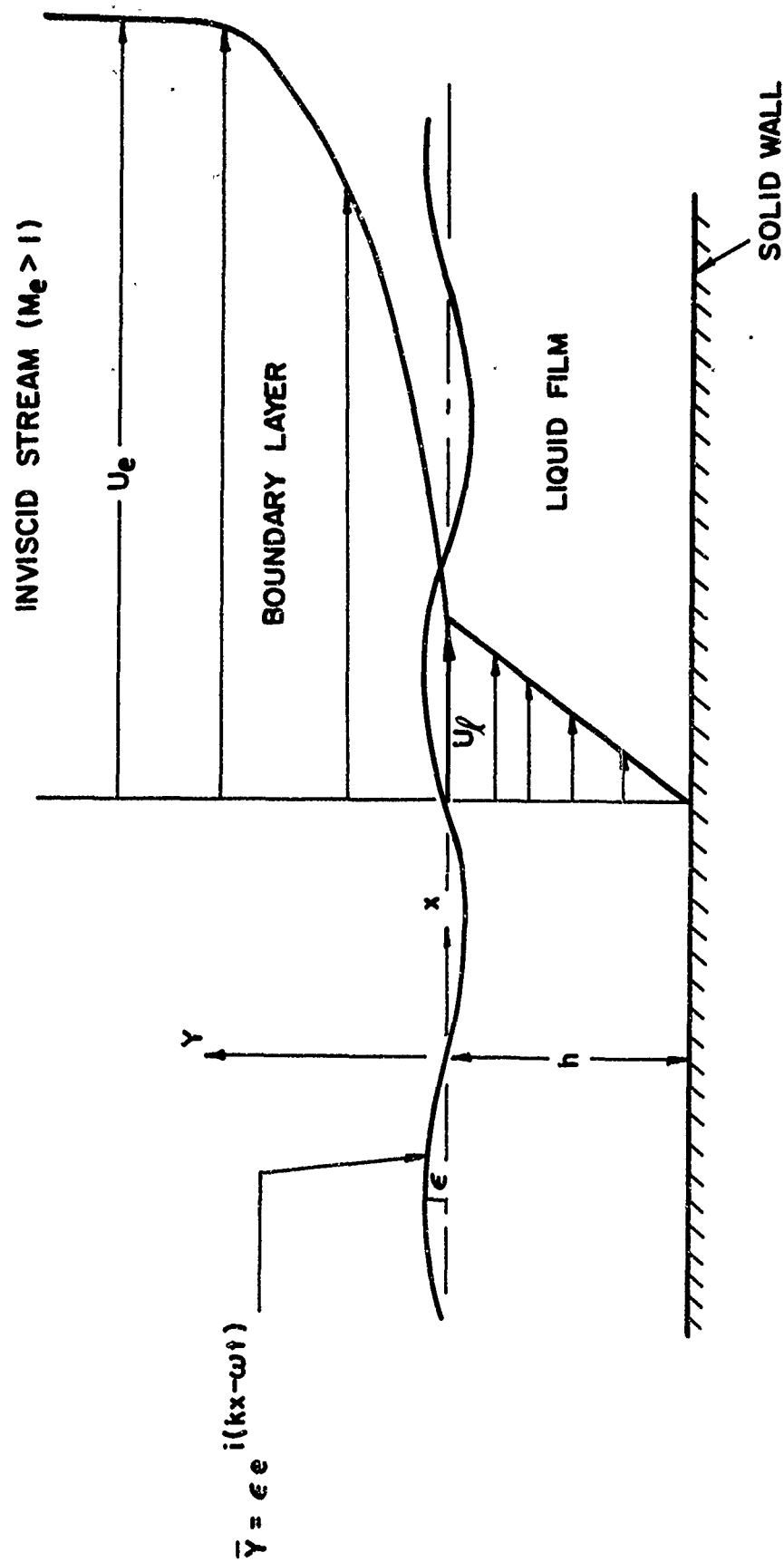
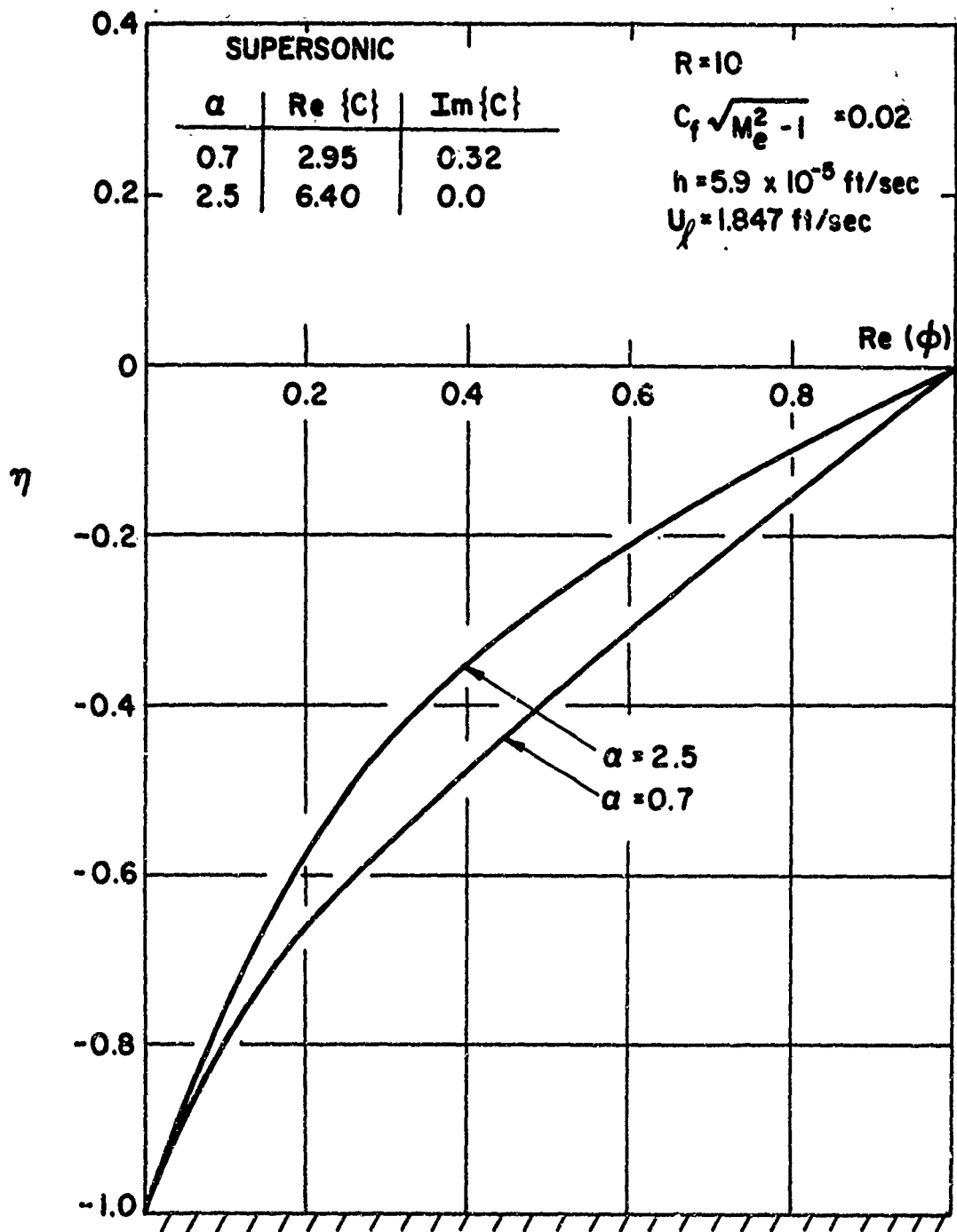


FIG.(1) FLOW CONFIGURATION



**FIG. (2a) BEHAVIOR OF THE EIGENFUNCTION:  
SUPERSONIC CASE**

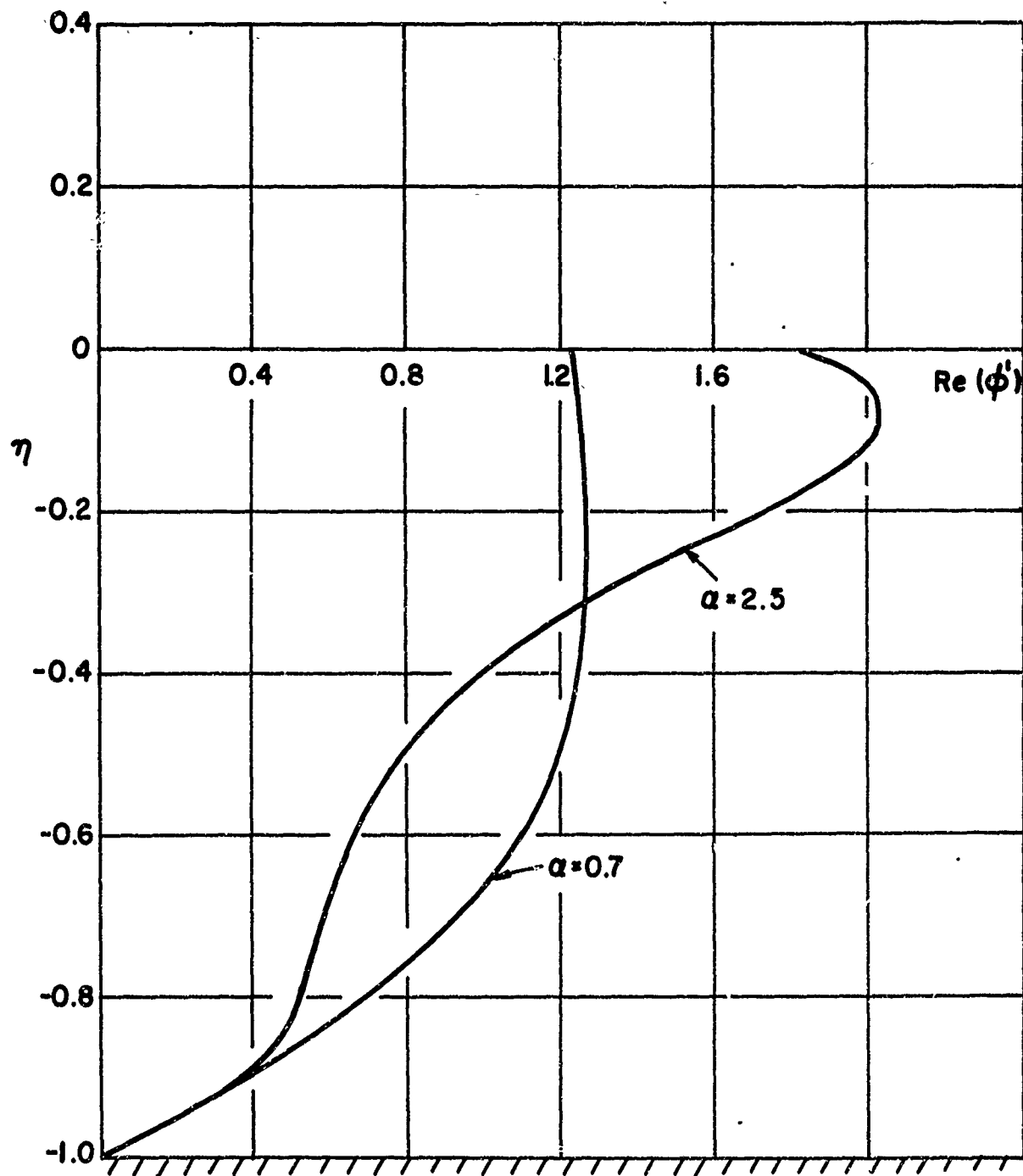


FIG. (2b) BEHAVIOR OF THE EIGENFUNCTION,  
SUPERSONIC CASE

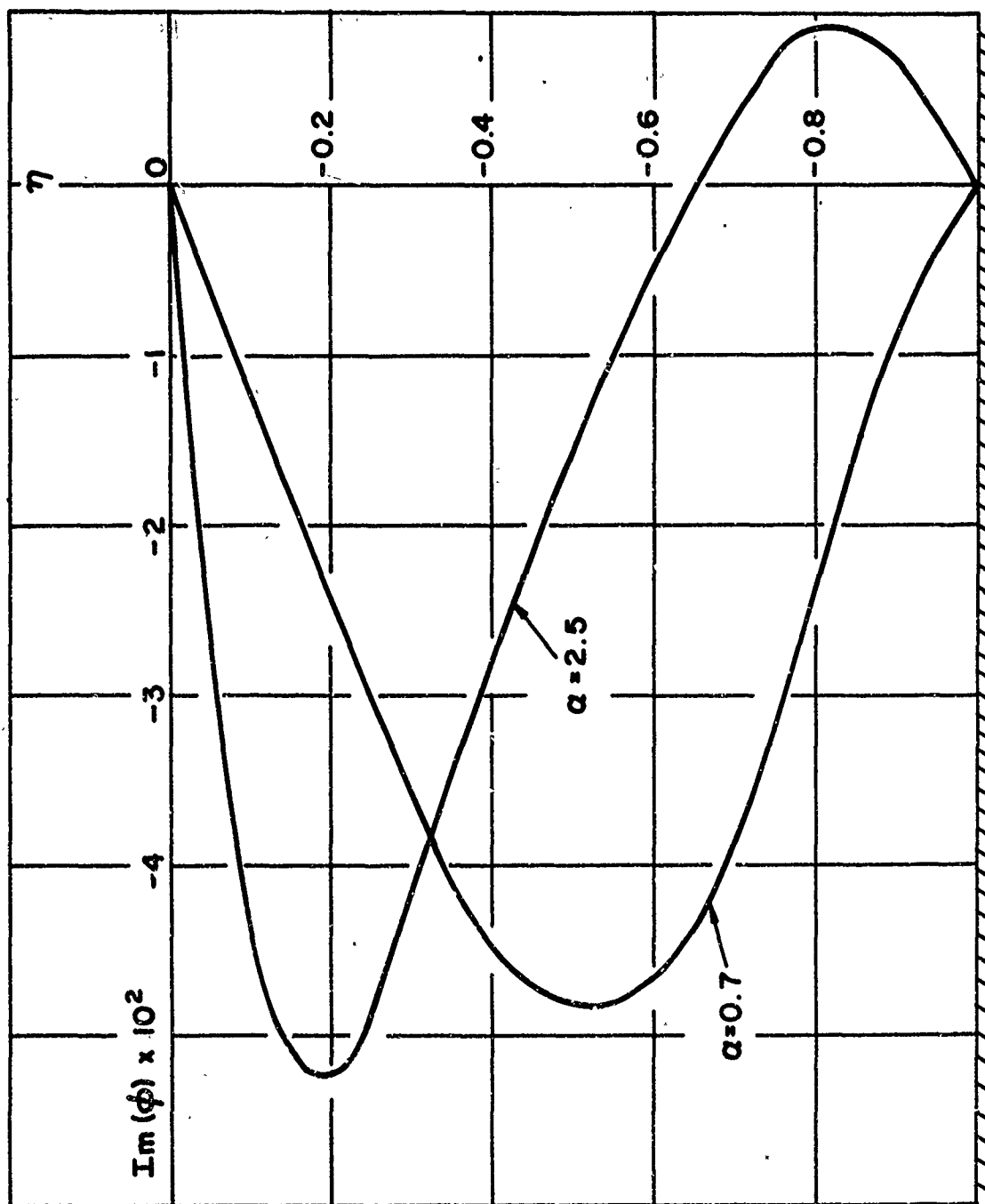


FIG. (2c) BEHAVIOR OF THE EIGENFUNCTION, SUPERSONIC CASE

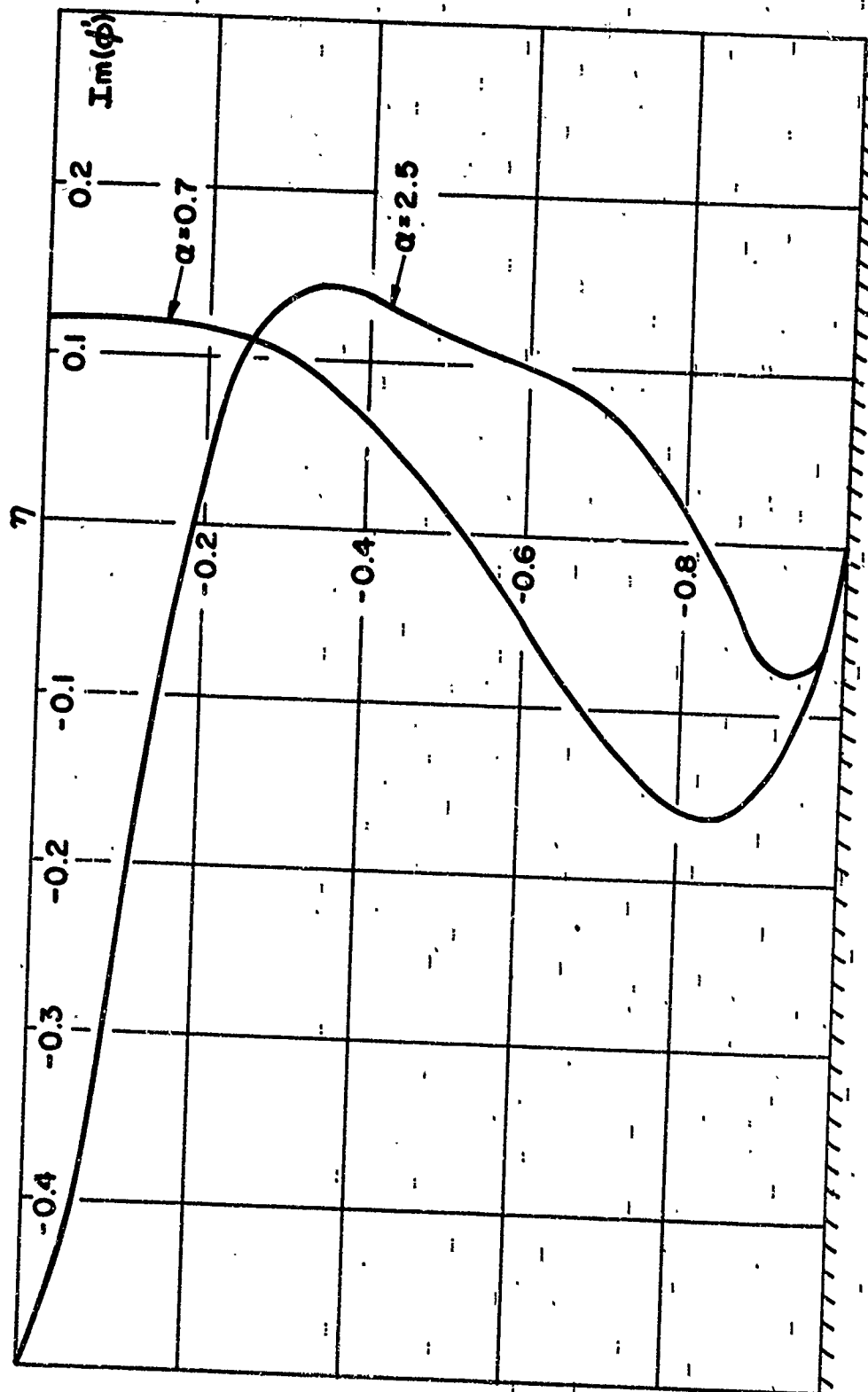


FIG. (2d) BEHAVIOR OF THE EIGENFUNCTION, SUPERSONIC CASE

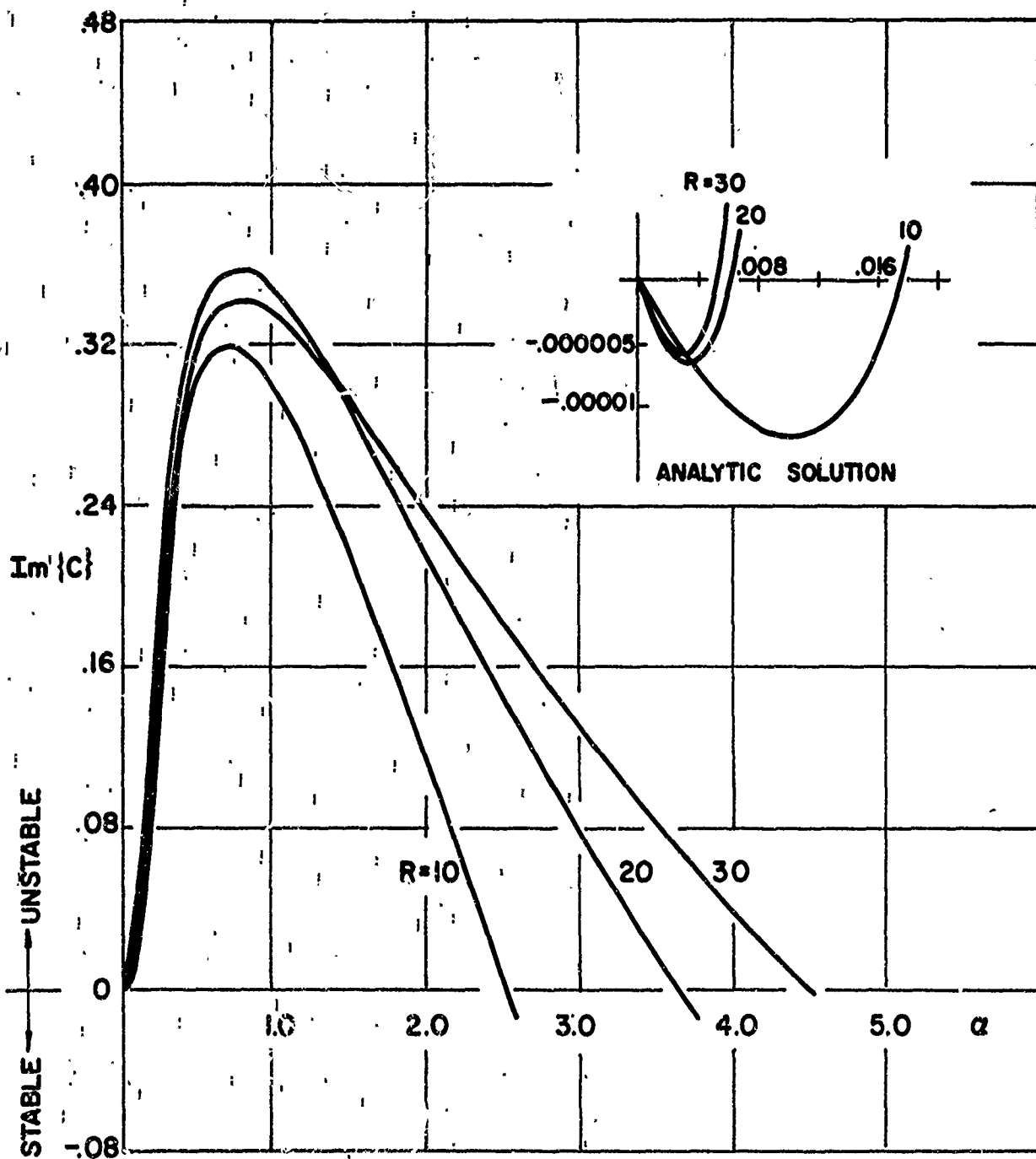


FIG. (3) WAVE AMPLIFICATION VS. WAVE NUMBER

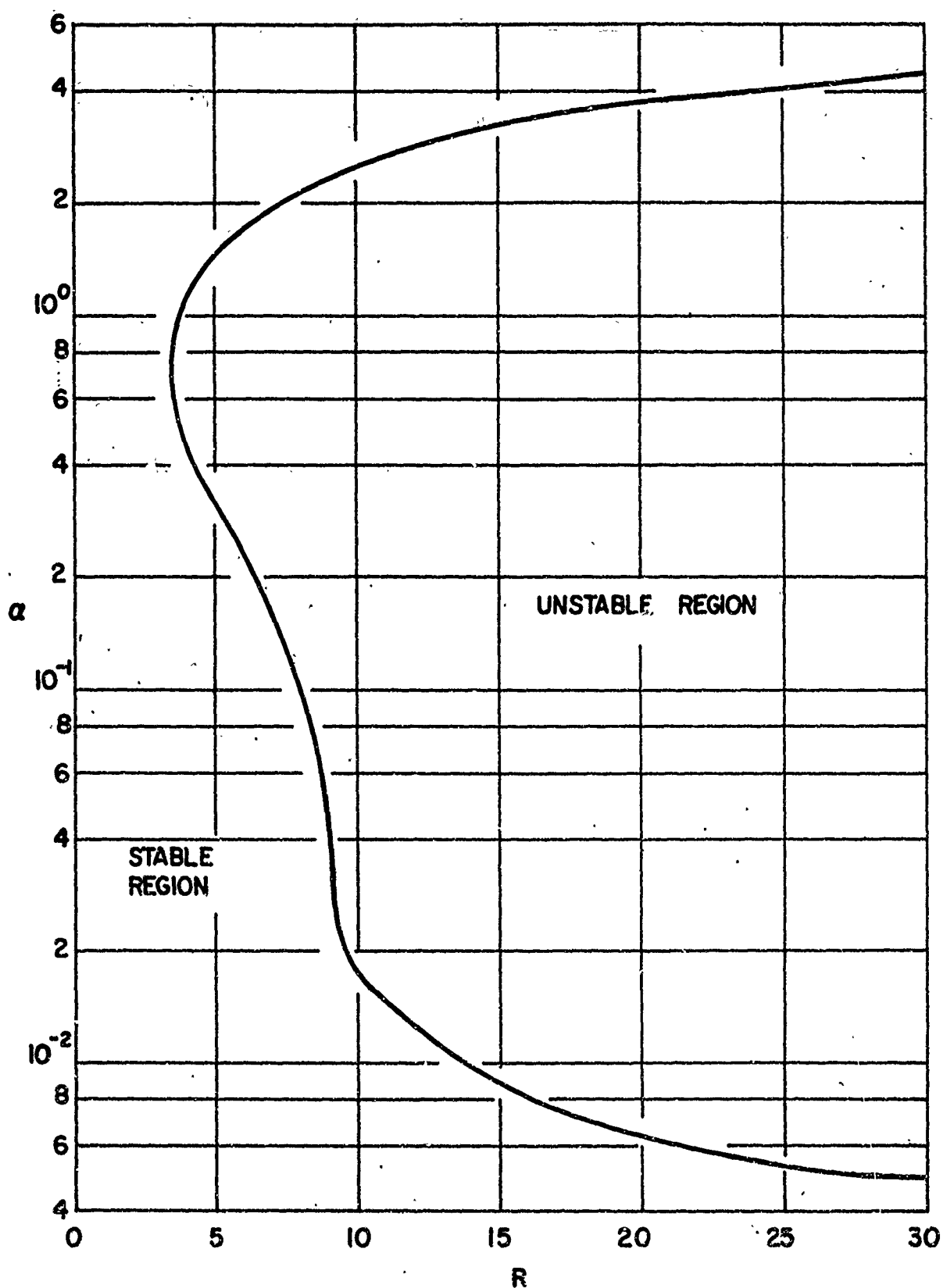


FIG. (4) CUT-OFF WAVE NUMBERS VS REYNOLDS NUMBER, SUPERSONIC CASE

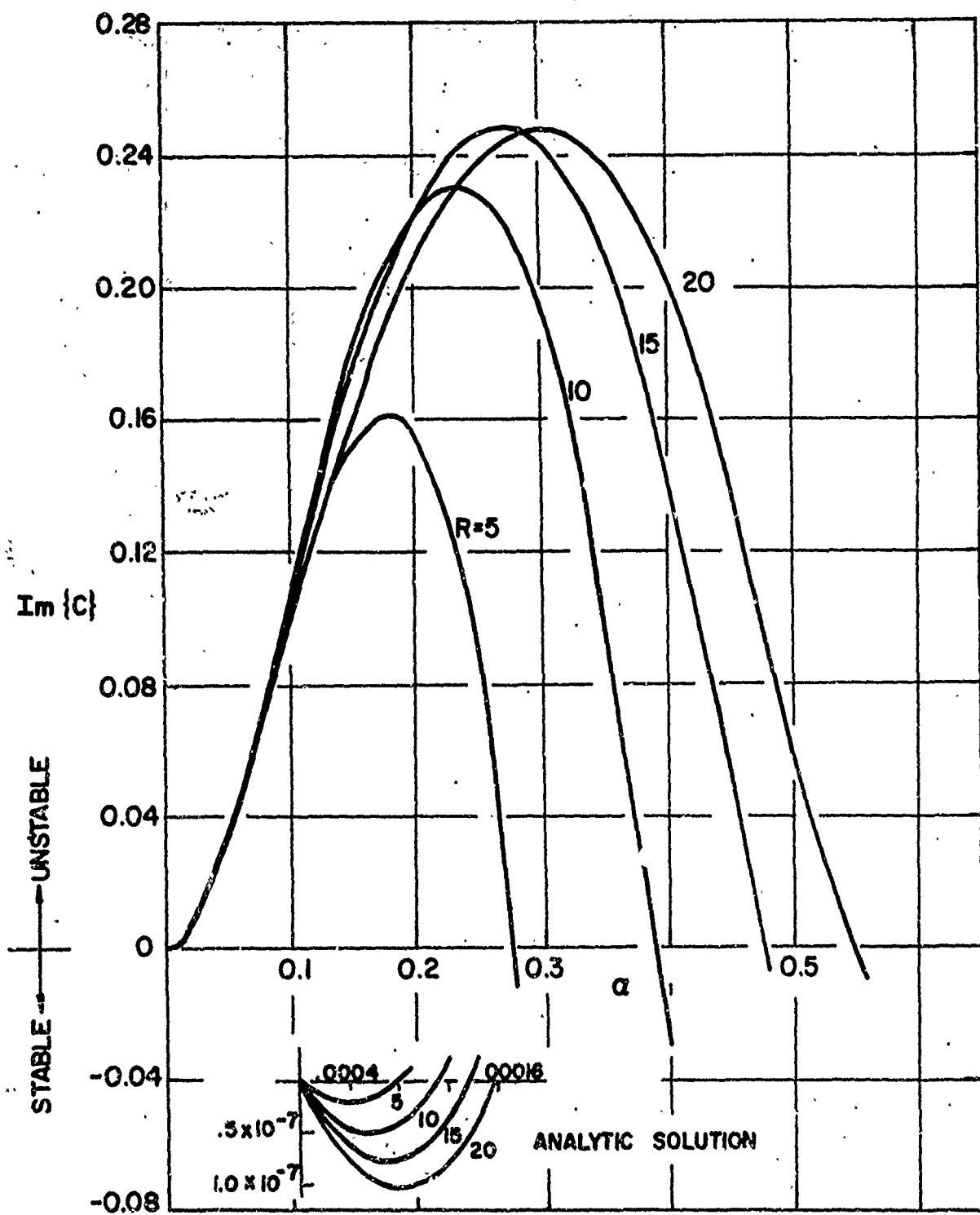


FIG. (5) AMPLIFICATION FACTOR VS WAVE NUMBER, SUBSONIC CASE



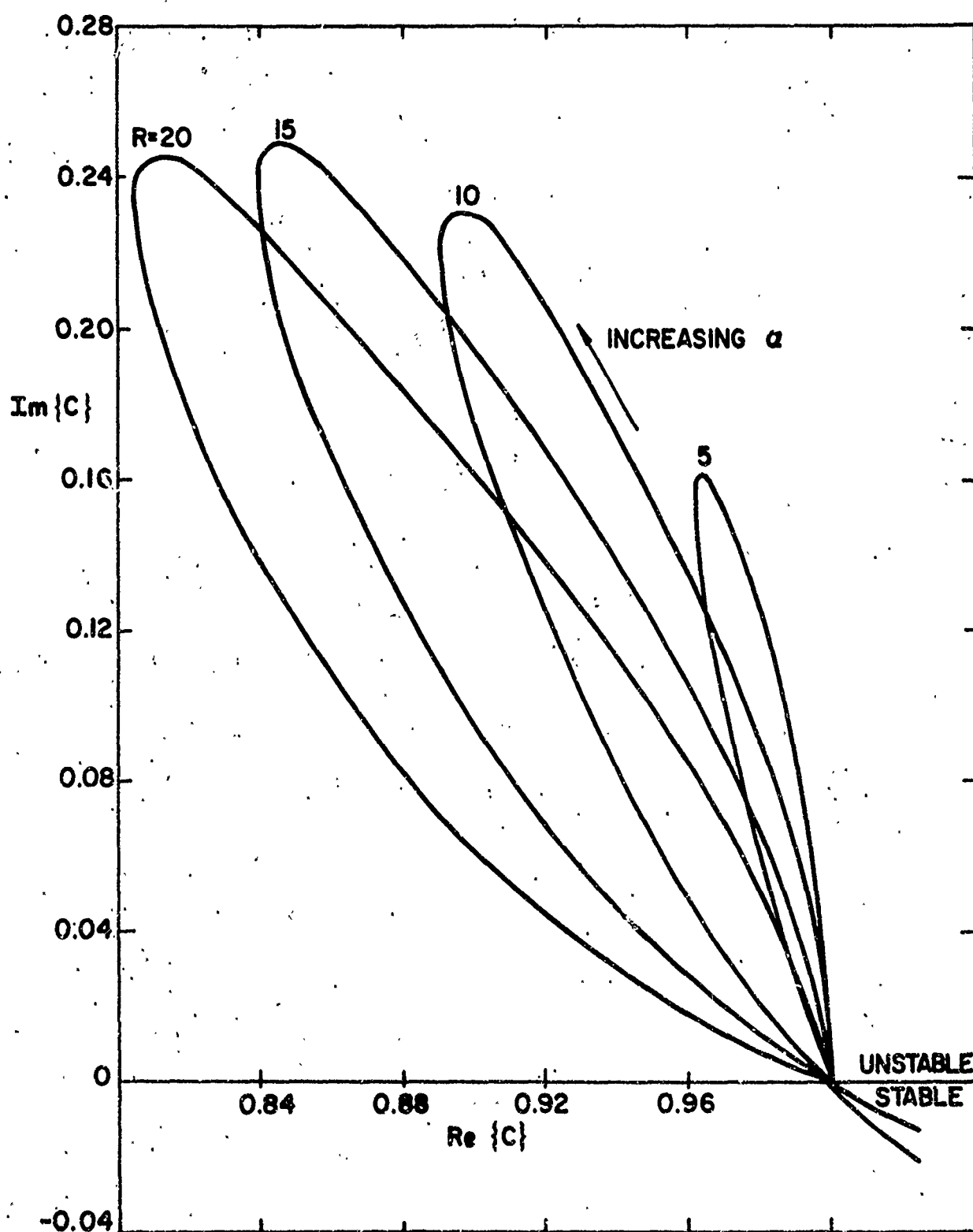


FIG. (6) AMPLIFICATION FACTOR VS WAVE SPEED  
FOR NEUTRAL STABILITY, SUBSONIC CASE

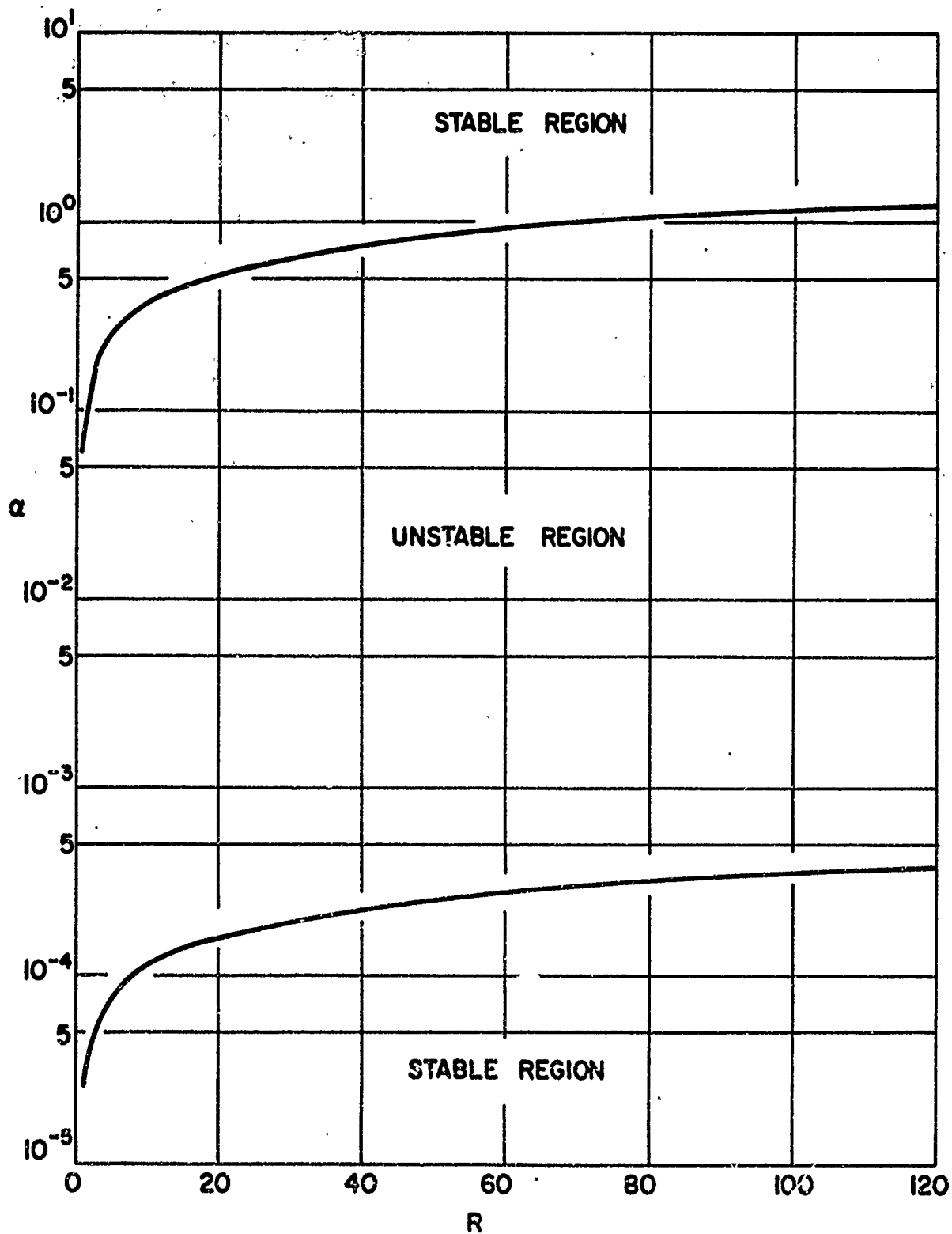


FIG.(7) CUT - OFF WAVE NUMBERS VS. REYNOLDS NUMBER, SUBSONIC CASE

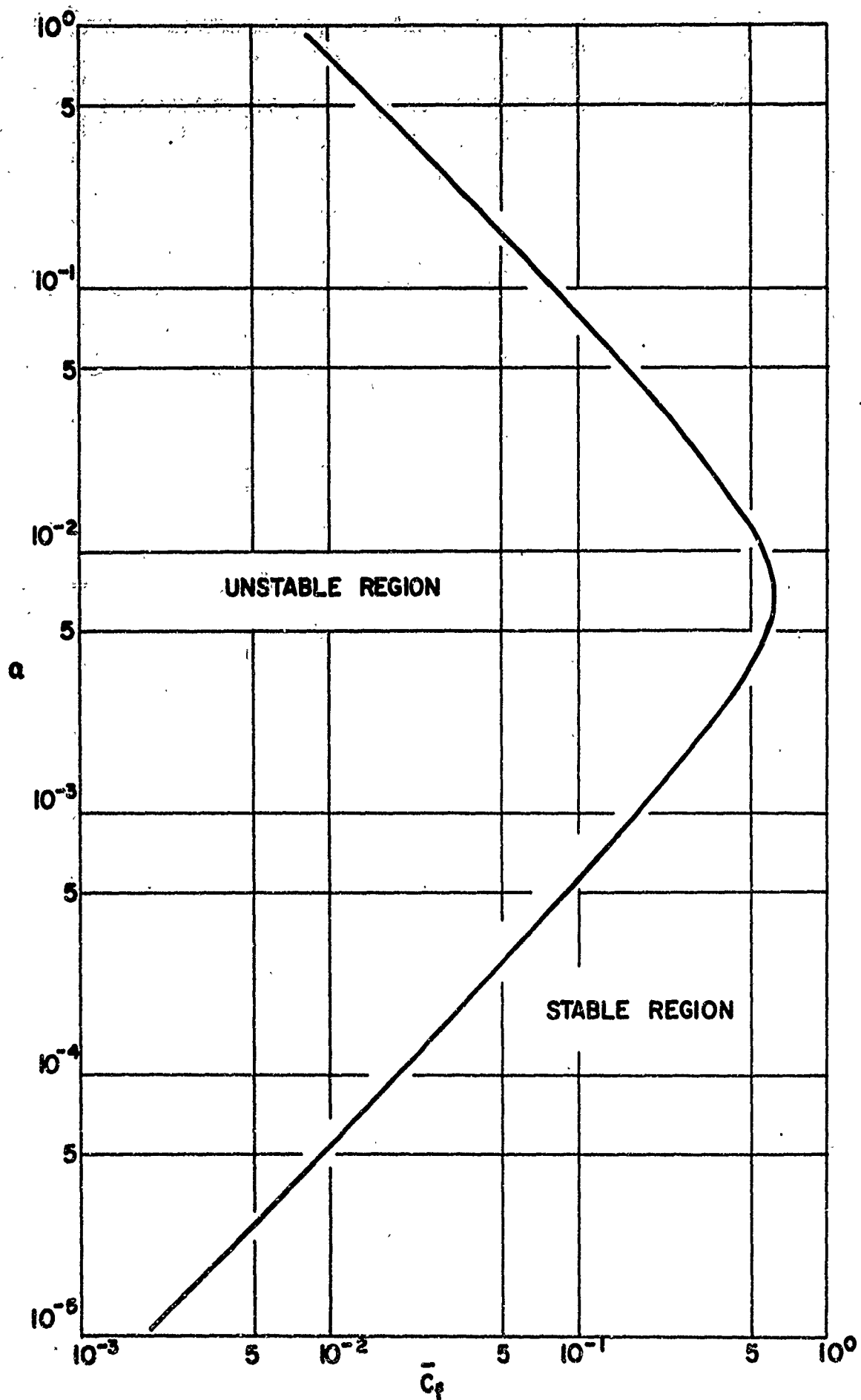


FIG. (8) CUT-OFF WAVE NUMBERS VS  $\bar{c}_f$ , SUBSONIC CASE,  $R=10$